

Cite this article as: Sun Dong, Wang Zhe, Jiang Shuyong, et al. Interface Compatibility During Different-Temperature Cu/NbTi Cladding Extrusion: Simulation and Experiment[J]. Rare Metal Materials and Engineering, 2023, 52(02): 441-447.

ARTICLE

# Interface Compatibility During Different-Temperature Cu/NbTi Cladding Extrusion: Simulation and Experiment

Sun Dong<sup>1,2</sup>, Wang Zhe<sup>3</sup>, Jiang Shuyong<sup>1,4</sup>, Zhang Yanqiu<sup>3</sup>

<sup>1</sup>Engineering Research Center of Advanced Metal Composites Forming Technology and Equipment, Ministry of Education, Taiyuan 030024, China; <sup>2</sup>College of Mechanical and Vehicle Engineering, Taiyuan University of Technology, Taiyuan 030024, China; <sup>3</sup>College of Mechanical and Electrical Engineering, Harbin Engineering University, Harbin 150001, China; <sup>4</sup>College of Materials Science and Engineering, Taiyuan University of Technology, Taiyuan 030024, China

**Abstract:** Different-temperature Cu/NbTi cladding extrusion was put forward where Cu and NbTi are different in temperature during plastic deformation. Different-temperature Cu/NbTi cladding extrusion can significantly lower the deformation temperature of Cu cladding layer so as to reduce the difference in yield stresses between Cu cladding layer and NbTi alloy core, which contributes to accommodating the deformation of the two metals. Rigid viscoplastic finite element method was used to simulate different-temperature Cu/NbTi cladding extrusion in order to reveal the interface compatibility between Cu cladding layer and NbTi alloy core, where various cone angles of bottom die, including 60°, 120° and 180°, were adopted. The results show that increasing the cone angle of bottom die contributes to reducing the relative elongation between Cu cladding layer and NbTi alloy core, which is conducive to the interface bonding between Cu cladding layer and NbTi alloy core. According to the optimal parameters from finite element simulation, Cu/NbTi cladding extrusion die with the cone angle of 180° can be used to implement Cu/NbTi cladding extrusion experiment. The experimental results show that stable flow of metal takes place during Cu/NbTi cladding extrusion, where Cu cladding layer and NbTi alloy core present compatible deformation and the relative elongation between them is small. The experimental results agree well with the simulated ones.

**Key words:** plastic deformation; extrusion; NbTi alloy; finite element method

NbTi alloys have attracted much attention as a class of functional alloys which depend on their chemical composition<sup>[1-3]</sup>. In general, NbTi alloy possesses shape memory effect when the content of Nb element is lower<sup>[4-7]</sup>. However, NbTi alloy belongs to a class of low-temperature superconducting material when the content of Nb element is higher<sup>[8-11]</sup>. As a superconducting alloy, NbTi alloy was commercially introduced 40 years ago, and NbTi alloy remains the only superconductor which is largely applied in magnet systems because it has good plasticity, mechanical processing properties and low-temperature superconducting properties<sup>[12]</sup>. The good plasticity of NbTi alloy makes it possible to produce the fine filamentary structure which is required in engineering application. Up to date, NbTi superconducting alloy has been widely used in

superconducting fields, such as nuclear magnetic resonance (NMR), international thermonuclear experimental reactor (ITER) conductor<sup>[13-14]</sup> and magnetic field concentrator<sup>[15]</sup>.

In fact, when it is used in the field of engineering, NbTi superconducting alloy generally is made into NbTi/Cu superconducting composite wires, where the NbTi alloy core is clad by the outer Cu layer<sup>[16-18]</sup>. In general, the superconducting joint which is used for connecting NbTi/Cu superconducting composite wires is also the product of Cu cladding NbTi alloy<sup>[19]</sup>. It is an effective method to process the superconducting joint based on Cu cladding NbTi rod. Therefore, it is a significant task to investigate the composite formability of Cu and NbTi alloy.

Guo et al<sup>[20]</sup> combined highly homogeneous Nb47Ti alloy with oxygen-free copper for fabricating NbTi/Cu wire which

Received date: May 18, 2022

Foundation item: National Natural Science Foundation of China (51871070)

Corresponding author: Jiang Shuyong, Ph. D., Professor, College of Materials Science and Engineering, Taiyuan University of Technology, Taiyuan 030024, P. R. China, E-mail: jiangshuyong@tyut.edu.cn

Copyright © 2023, Northwest Institute for Nonferrous Metal Research. Published by Science Press. All rights reserved.

possesses low copper-to-superconductor ratio of 1.3 and a filament number of 630 and proposed a new heat treatment method to enhance the critical current density. Park et al.<sup>[21]</sup> fabricated NbTi/Cu superconducting composite wires by combining equal channel angular pressing with subsequent groove rolling and drawing, and found that repetitive large plastic deformation and intermediate heat treatments can lead to the high volume fraction of  $\alpha$ -Ti precipitates at grain boundary intersections, which contributes to enhancing the critical current density in the lower range of magnetic field. Cheng et al.<sup>[22]</sup> used electromagnetic forming technology to prepare NbTi superconducting joint which consists of a copper outer tube and a NbTi alloy inner column and found that electromagnetic formed NbTi superconducting joint has low resistance as well as excellent electrical conductivity. Stolyarov<sup>[23]</sup> obtained monofilamentary and multifilamentary Cu/NbTi composite superconductors by means of rolling with the help of pulse current and found that rolling with current obviously contributes to enhancing plastic deformation ability of Cu/NbTi composite superconductors.

In the present study, different-temperature Cu/NbTi cladding extrusion was put forward and interface compatibility of Cu and NbTi samples was investigated based on finite element simulation and experiment. This work will help to understand the fabrication mechanism of Cu/NbTi composite superconductors in the extrusion process.

## 1 Finite Element Simulation

### 1.1 FEM of Cu/NbTi cladding extrusion

Finite element model (FEM) of Cu/NbTi cladding extrusion is shown in Fig. 1, where Cu cladding layer is 10 mm in the outer diameter, 6 mm in inner diameter and, 20 mm in length, and NbTi alloy core is 6 mm in diameter and 20 mm in length. Three-dimension model of Cu/NbTi cladding extrusion was established by UG NX 10.0 software. The involved three-dimension model was put into DEFORM finite element code, where the Cu sample and the NbTi sample were divided into 60 000 meshes. The former possesses 14 570 nodes and the latter possesses 12 592 nodes. Lagrangian incremental simulation method was selected in the DEFORM software, where conjugate-gradient solver and direct iteration method were adopted.

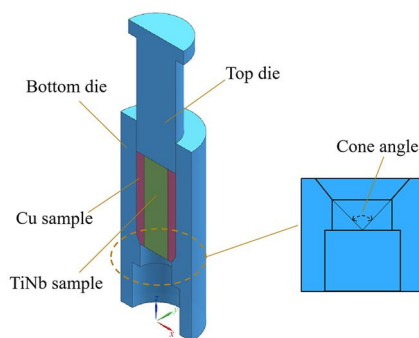


Fig.1 Finite element model of Cu/NbTi cladding extrusion

### 1.2 Establishment of boundary condition

#### (1) Temperature boundary condition

Deformation temperature has a pronounced impact on Cu/NbTi cladding extrusion because yield stress of metal materials decreases with the increase in deformation temperature. It is evident that yield stress of Cu sample is obviously lower than that of NbTi alloy when their deformation temperatures are the same. Therefore, during finite element simulation of Cu/NbTi cladding extrusion, the temperature of the Cu/NbTi billet was set as 800 °C, whereas that of the dies was set as room temperature. In other words, die heating was not considered during extrusion. Consequently, Cu cladding layer firstly touched the bottom die and thus the temperature of Cu cladding layer was lowered due to the action of heat transfer. The temperature difference between Cu cladding layer and NbTi alloy core contributes to reducing the yield stress between the two samples, which plays an important role in enhancing the deformation compatibility between Cu cladding layer and NbTi alloy core.

#### (2) Friction boundary condition

Friction boundary condition has an important influence on Cu/NbTi cladding extrusion. NbTi alloy core was assembled into Cu cladding layer by interference fit. The friction coefficient between Cu cladding layer and NbTi alloy core was set as 0.99 during finite element simulation of Cu/NbTi cladding extrusion in order to restrict the relative movement between Cu cladding layer and NbTi alloy core. The friction coefficient between Cu/NbTi billet and die was determined as 0.3.

#### (3) Velocity boundary condition

During Cu/NbTi cladding extrusion, the extrusion velocity was set as 1 mm/s at the boundary where Cu/NbTi cladding billet touched the top die. The initial extrusion velocity was defined as 0 mm/s at the free end of Cu/NbTi cladding billet.

### 1.3 Constitutive model of materials

The constitutive models of NbTi alloy and Cu sample were established based on Arrhenius type constitutive equation. Therefore, the constitutive equation of NbTi alloy is established as follows<sup>[24]</sup>.

$$\dot{\epsilon} = 1.71354 \times 10^{12} \left[ \sinh(1.1264 \times 10^{-2} \sigma) \right]^{6.5231} \exp\left(\frac{-3.06381 \times 10^5}{RT}\right) \quad (1)$$

The constitutive equation of Cu sample is established as follows<sup>[25]</sup>.

$$\dot{\epsilon} = e^{22.483} \left[ \sinh(1.734 \times 10^{-2} \sigma) \right]^{5.3152} \exp\left(\frac{-2.09455 \times 10^5}{RT}\right) \quad (2)$$

Eq. (1) and Eq. (2) shall be used as constitutive models of materials during finite element simulation of Cu/NbTi cladding extrusion. In addition, physical parameters of NbTi alloy and Cu sample are shown in Table 1. The dies are set as rigid bodies.

### 1.4 Finite element simulation parameters

In the present study, cone angles of bottom die were selected as process variables during finite element simulation

**Table 1** Physical parameters of NbTi alloy and Cu sample

Physical parameter	NbTi	Cu
Thermal conductivity/ $W \cdot m^{-1} \cdot K^{-1}$	12	339
Young's modulus/GPa	56	71
Poisson's ratio	0.33	0.35
Specific heat capacity/ $J \cdot kg^{-1} \cdot K^{-1}$	523	385
Emissivity	0.7	0.15
Coefficient of linear expansion	10	17

of Cu/NbTi cladding extrusion in order to investigate the influence of cone angle on the formability of Cu/NbTi cladding extrusion products. Cone angles of bottom die were chosen as  $60^\circ$ ,  $120^\circ$  and  $180^\circ$ . The friction coefficient between Cu/NbTi billet and die was determined as 0.3. Extrusion velocity was determined as 1 mm/s.

## 2 Results and Discussion

### 2.1 Distribution of temperature field

Fig. 2 shows temperature field distribution of Cu/NbTi cladding extrusion based on finite element simulation. It can be found that there is an obvious temperature decrease in the contact zone where NbTi alloy core touches top die, whereas there is no apparent temperature reduction in the remaining section of NbTi alloy core. However, Cu cladding layer shows a relatively larger temperature decrease because the corresponding outer layer metal is completely in contact with

the die whose temperature was set as room temperature. Fig.2d shows the temperature variation curves of Cu cladding layer at cone angles of  $60^\circ$ ,  $120^\circ$  and  $180^\circ$ , where the abscissa is the distance from bottom to top of Cu/NbTi coated extruded products.

### 2.2 Distribution of stress field

Fig. 3 shows effective stress distribution of Cu/NbTi cladding extrusion based on finite element simulation at cone angles of  $60^\circ$ ,  $120^\circ$  and  $180^\circ$ . It is generally accepted that effective stress is an important factor reflecting plastic deformation of metal materials, where plastic deformation can take place only when effective stress is equal to yield stress according to Von Mises yield criterion. It can be observed from Fig. 3 that in the plastic deformation zone, effective stress of TiNb alloy core is higher than that of Cu cladding layer. However, as for plastic deformation of Cu cladding layer, effective stress of the outer layer is greater than that of the inner layer.

Fig. 4 shows stress distribution of Cu/NbTi cladding extrusion based on finite element simulation at cone angles of  $180^\circ$ . It can be found that there is a three-dimensional compressive state in the deformation zone of Cu cladding layer, where radial stress, tangential stress and axial stress are compressive stresses. However, in the deformation zone of NbTi alloy core, radial stress and tangential stress are compressive stresses, and axial stress belongs to tensile stress. It is well known that plastic deformation zone is always in a

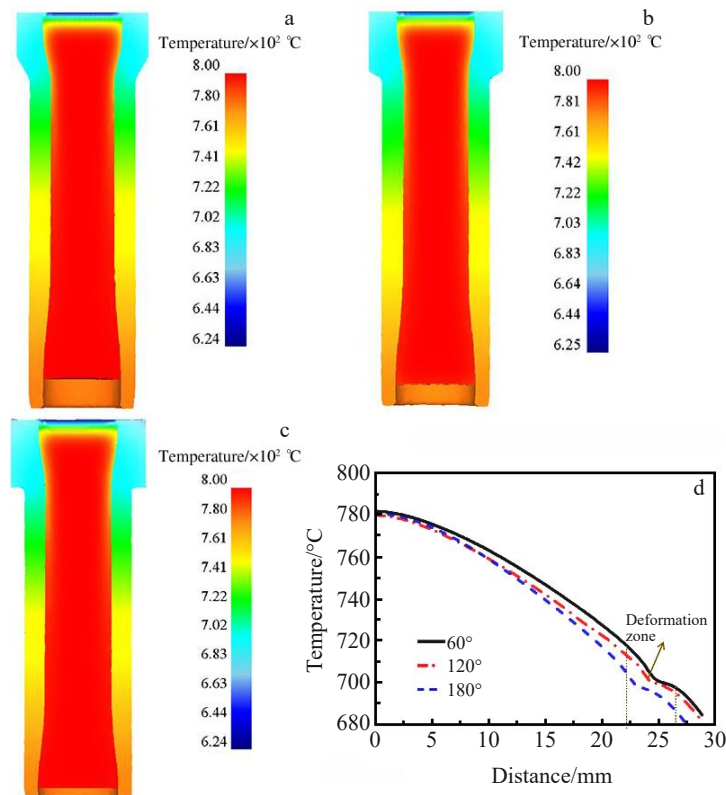


Fig.2 Temperature field variation of Cu/NbTi cladding extrusion with various cone angles of  $60^\circ$  (a),  $120^\circ$  (b), and  $180^\circ$  (c) for bottom Cu cladding layer (d)

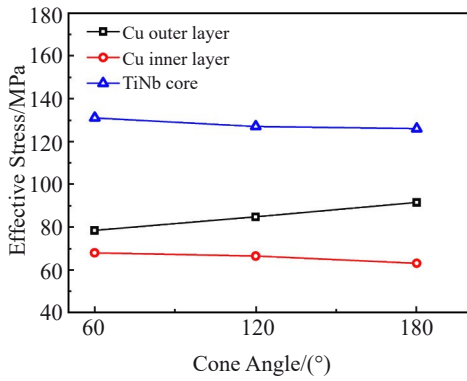


Fig.3 Variation of effective stress with cone angle in deformation zone during Cu/NbTi cladding extrusion

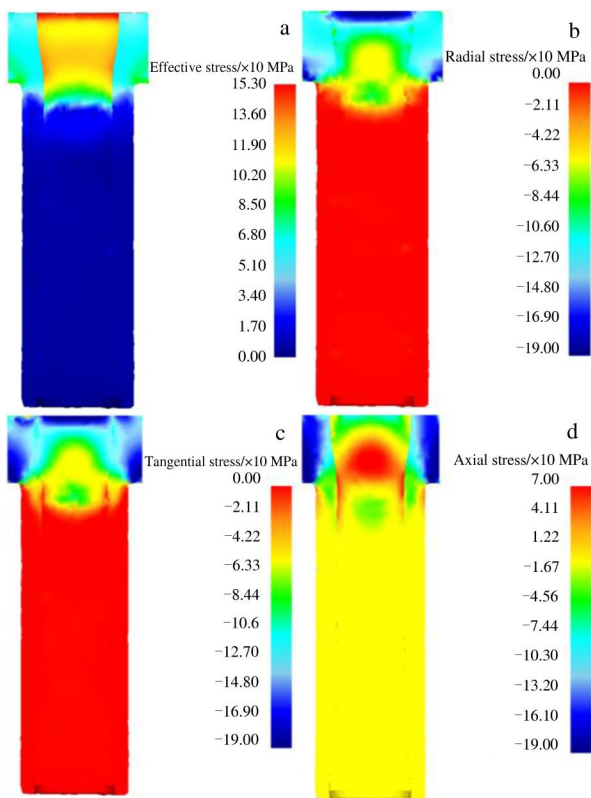


Fig.4 Stress distribution of Cu/NbTi cladding extrusion at cone angle of 180°: (a) effective stress, (b) radial stress, (c) tangential stress, and (d) axial stress

three-dimensional compressive stress state in the conventional extrusion process. However, during Cu/NbTi cladding extrusion, flow velocity of Cu cladding layer is not consistent with that of NbTi alloy core, and the former is obviously higher than the latter. Therefore, when Cu cladding layer is subjected to plastic deformation, tensile stress is induced in the deformation zone of NbTi alloy core due to the action of the friction force between Cu cladding layer and NbTi alloy core. It is evident that the tensile stress makes the plastic deformation zone easier to satisfy yield criterion.

2.3 Distribution of strain field

Fig. 5 indicates effective strain distribution of Cu/NbTi cladding extrusion based on finite element simulation at cone angles of 60°, 120° and 180°. It can be obviously observed that the effective strain of the outer layer is greater than that of the inner layer in the deformation zone of Cu cladding layer, and the effective strain in the deformation zone of NbTi alloy core is relatively lower. In particular, the effective strain in the outer layer of Cu sample increases considerably with the increase in cone angle. However, as for the inner layer of Cu sample and NbTi alloy core, the effective strain shows a very small variation with the increase in cone angle. The phenomenon indicates that the increase in cone angle leads to the substantially inhomogeneous plastic deformation of Cu cladding layer.

Fig.6 shows strain distribution of Cu/NbTi cladding extrusion based on finite element simulation at the cone angle of 180°. For the purpose of revealing strain distribution characteristic of Cu/NbTi cladding extrusion, Cu/NbTi cladding extrusion sample can be divided into three zones, including steady flow zone, plastic deformation zone and extrusion exit end. In the steady flow zone, Cu cladding layer and NbTi alloy present almost similar strain distribution characteristics, where radial strain and tangential strain belong to compressive strain, whereas axial strain is tensile strain. However, in the plastic deformation zone, Cu cladding layer and NbTi alloy core exhibit different strain distribution characteristics. In the plastic deformation zone of Cu cladding layer, radial strain and axial strain belong to tensile strain, but tangential strain belongs to compressive strain. However, in the plastic deformation zone of NbTi alloy core, radial strain and tangential strain belong to compressive strain, but axial strain belongs to tensile strain.

As for extrusion exit end, in particular, NbTi alloy core exhibits a horn-like shape. In fact, at the initial stage of extrusion, the exit end of Cu/NbTi cladding extrusion billet belongs to the free end without any constraint, where plastic deformation degree is very small. This is one reason why the horn-like shape is formed. In addition, during Cu/NbTi cladding extrusion, the extrusion exit end of NbTi alloy core is

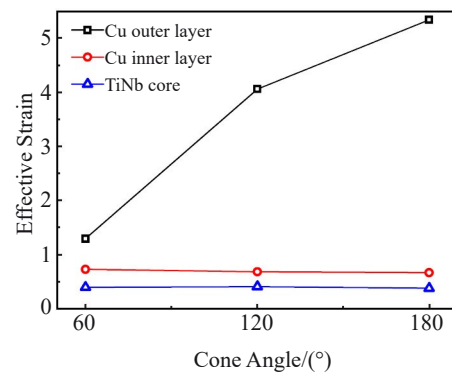


Fig.5 Variation of effective strain with cone angle in deformation zone during Cu/NbTi cladding extrusion

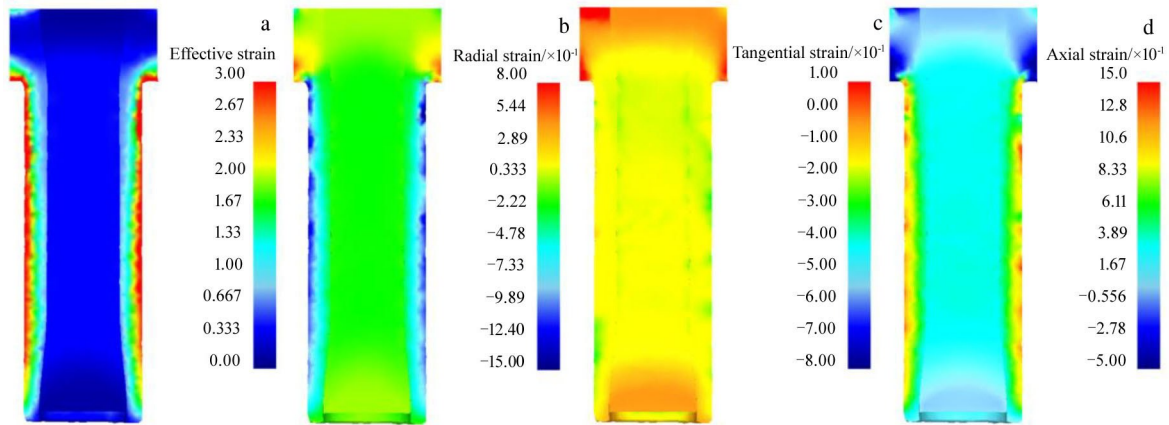


Fig.6 Strain distribution of Cu/NbTi cladding extrusion at the cone angle of 180°: (a) effective strain, (b) radial strain, (c) tangential strain, and (d) axial strain

subjected to compressive strain in the radial and tangential directions as well as tensile strain in the axial direction, and simultaneously it experiences shear deformation due to the action of friction. The shear deformation decreases gradually from outer layer to inner layer of metal. At the initial stage of extrusion, the extrusion exit end of NbTi alloy core is subjected to very small shear deformation. Shear deformation increases gradually with the extrusion stroke proceeding. The horn-like shape is formed at the extrusion exit end when TiNb alloy core is at the stage of stable flow.

In summary, cone angle has a great effect on plastic

deformation of Cu cladding layer. The increase in cone angle leads to more inhomogeneous plastic deformation of Cu cladding layer, where the difference in the strain values between the inner layer and the outer layer becomes larger and larger.

#### 2.4 Distribution of velocity field

Fig.7 shows velocity field distribution of Cu/NbTi cladding extrusion based on finite element simulation at cone angles of 60°, 120° and 180°. It can be found that at the stage of steady flow, velocity field is basically homogeneous in Cu cladding layer and TiNb alloy core. Furthermore, when cone angle is

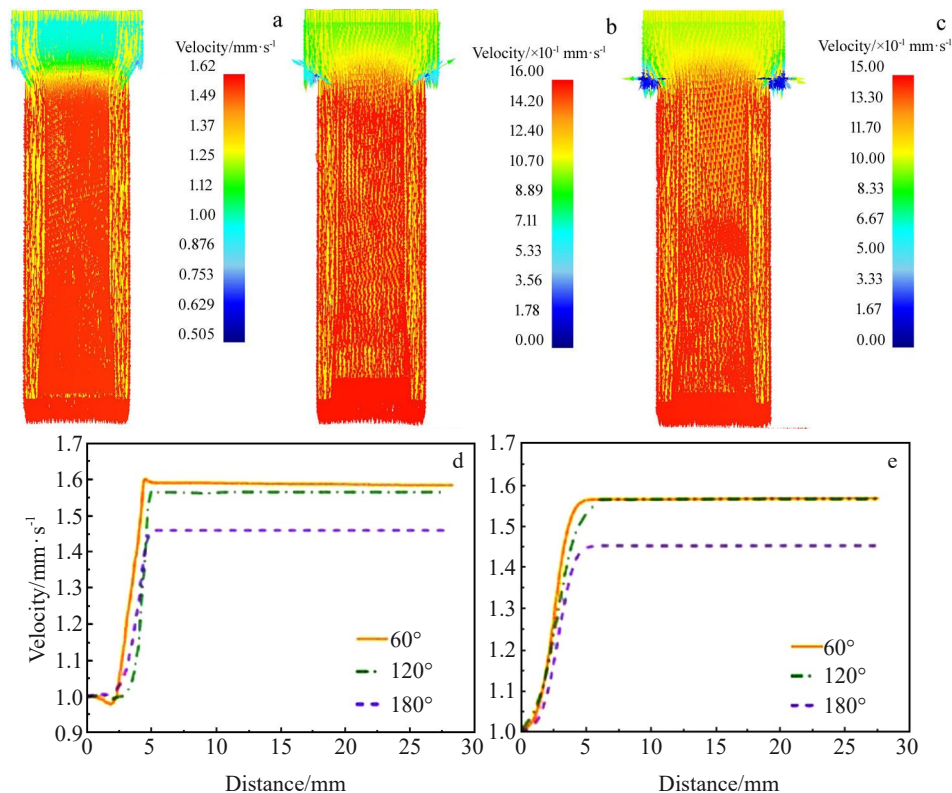


Fig.7 Velocity field variation of Cu/NbTi cladding extrusion with cone angles of 60° (a), 120° (b), and 180° (c); velocity variation curves of Cu cladding layer (d) and NbTi alloy core (e)

increased from  $60^\circ$  to  $120^\circ$ , extrusion velocity of Cu cladding layer slightly decreases, whereas extrusion velocity of NbTi alloy core is unchangeable. However, when cone angle increases to  $180^\circ$ , the extrusion velocity of Cu cladding layer and NbTi alloy core is considerably lowered. In particular, the relative extrusion velocity between Cu cladding layer and NbTi alloy core is obviously reduced. In other words, the cone angle of  $180^\circ$  considerably restricts the flow of Cu cladding layer during Cu/NbTi cladding extrusion. When cone angles are  $60^\circ$ ,  $120^\circ$  and  $180^\circ$ , the relative displacement values between Cu cladding layer and TiNb alloy core are 2.3, 1.2 and 0.55 mm, respectively. It is evident that the cone angle of  $180^\circ$  contributes to the deformation compatibility between Cu cladding layer and NbTi alloy core.

### 3 Experimental Validation

According to the aforementioned finite element simulation results, it can be found that elongation of Cu cladding layer is obviously greater than that of NbTi alloy core during Cu/NbTi cladding extrusion. In other words, the incompatible deformation between Cu cladding layer and NbTi alloy core takes place. It is necessary to restrict the flow of Cu cladding layer during Cu/NbTi cladding extrusion in order to guarantee the deformation compatibility between Cu cladding layer and NbTi alloy core. One measure is taken to increase the cone angle so as to restrict the flow of Cu cladding layer. Another measure is taken to enhance the friction between Cu cladding layer and die, which contributes to constraining the flow of Cu cladding layer.

According to the optimal parameters based on finite element simulation, Cu/NbTi cladding extrusion die is designed, where the cone angle of bottom die is determined as  $180^\circ$ , as shown in Fig.8. The dimension of Cu/NbTi cladding extrusion billet is completely consistent with finite element model, as shown in Fig. 9. Cu/NbTi cladding extrusion experiment is carried out in the case of no lubrication. Cu/NbTi cladding billet is heated to  $800^\circ\text{C}$  during extrusion experiment and then put into extrusion die. The experimental results show that stable flow of metal takes place during Cu/NbTi cladding extrusion, where Cu cladding layer and NbTi

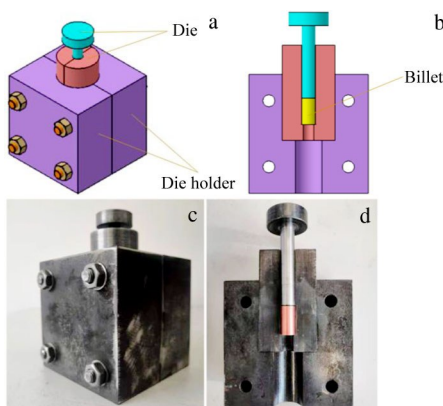


Fig.8 Three-dimensional models (a, b) and real photographs (c, d) of Cu/NbTi cladding extrusion die

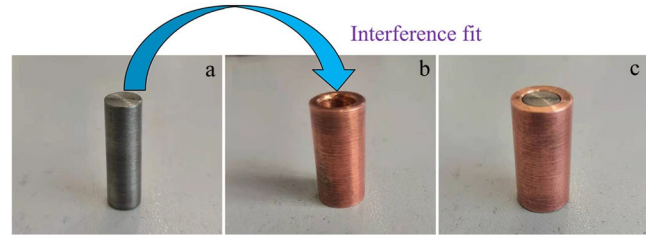


Fig. 9 Real photographs of Cu/NbTi cladding extrusion billet: (a) NbTi, (b) Cu, and (c) Cu/NbTi billet

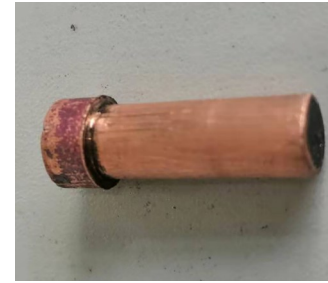


Fig.10 Real photograph of Cu/NbTi sample after cladding extrusion

alloy core present compatible deformation and they do not almost exhibit the relative elongation, as shown in Fig.10. The experimental results agree well with the simulated ones.

### 4 Conclusions

1) Different-temperature Cu/NbTi cladding extrusion is put forward, i.e. Cu and NbTi are different in temperature during plastic deformation. Different-temperature Cu/NbTi cladding extrusion can significantly lower the deformation temperature of Cu cladding layer so as to reduce the difference in yield stresses between Cu cladding layer and NbTi alloy core, which contributes to accommodating the deformation of the two metals. Various cone angles of bottom die are selected as finite element parameters to investigate the interface compatibility between Cu cladding layer and NbTi alloy core.

2) Finite element simulation results show that cone angles of bottom die have no considerable influence on the distributions of temperature field and stress field, whereas they have a substantial influence on the distributions of strain field and velocity field. Increasing cone angles of bottom die leads to inhomogeneous plastic deformation of Cu cladding layer, where the outer layer shows a larger strain value, and the inner layer exhibits a smaller strain value. In addition, increasing cone angles of bottom die contributes to restricting the flow of Cu cladding layer to guarantee the deformation compatibility between Cu cladding layer and NbTi alloy core.

3) According to the optimal parameters based on finite element simulation, Cu/NbTi cladding extrusion experiment is carried out in the case of no lubrication, where cone angle of bottom die is determined as  $180^\circ$ . The dimension of Cu/NbTi cladding extrusion billet is designed according to the finite element model. The experimental results show that stable flow

of metal takes place during Cu/NbTi cladding extrusion, where Cu cladding layer and NbTi alloy core present compatible deformation and they do not exhibit the relative elongation. The experimental results agree well with the simulated ones.

## References

- 1 Mathebula C, Matizanhuka W, Bolokang A S. *The International Journal of Advanced Manufacturing Technology*[J], 2020, 108: 23
- 2 Gehring D, Monroe J A, Karaman I. *Scripta Materialia*[J], 2020, 178: 351
- 3 Al-Zain Y, Kim H Y, Miyazaki S. *Materials Science and Engineering A*[J], 2015, 644: 95
- 4 Sun B, Meng X L, Gao Z Y et al. *Journal of Alloys and Compounds*[J], 2017, 715: 16
- 5 Okulov I V, Volegov A S, Attar H et al. *Journal of the Mechanical Behavior of Biomedical Materials*[J], 2017, 65: 866
- 6 Ibrahim M K, Hamzah E, Saud S N et al. *Transactions of Nonferrous Metals Society of China*[J], 2018, 28(4): 700
- 7 Helth A, Pilza S, Kirstena T et al. *Journal of the Mechanical Behavior of Biomedical Materials*[J], 2017, 65: 137
- 8 Santra S, Davies T, Matthews G et al. *Materials & Design*[J], 2019, 176: 107 836
- 9 Nijhuis A, Ilyin Y, Abbas W et al. *Cryogenics*[J], 2004, 44(5): 319
- 10 Bruzzone P, Stepanov B, Zapretalina E. *Fusion Engineering and Design*[J], 2005, 75-79: 111
- 11 Mousavi T, Grant P S, Speller S C et al. *Materials Design*[J], 2021, 198: 109 285
- 12 Wilson M N. *Cryogenics*[J], 2008, 48(7-8): 381
- 13 Li J F, Zhang P X, Liu X H et al. *Physica C: Superconductivity and Its Applications*[J], 2008, 468: 1840
- 14 Nannini M, Cloez H, Girar S et al. *Fusion Engineering and Design*[J], 2009, 84: 1404
- 15 Zhang Z Y, Matsumoto S, Choi S et al. *Physica C: Superconductivity and Its Applications*[J], 2011, 471: 1547
- 16 Li J F, Zhang P X, Liu X H et al. *Physica C: Superconductivity and Its Applications*[J], 2008, 468(15-20): 1840
- 17 Somerkoski J, Zignani C F, Marzi G D et al. *Physics Procedia*[J], 2012, 36(1): 1516
- 18 Guan M, Wang X Z, Zhou Y H. *SpringerPlus*[J], 2015, 4: 81
- 19 Zhou F, Cheng J S, Dai Y M et al. *Physica C: Superconductivity and Its Applications*[J], 2014, 498: 9
- 20 Guo Q, Zhang P X, Feng Y et al. *Rare Metal Materials and Engineering*[J], 2019, 48(12): 4113 (in Chinese)
- 21 Park S M, Oh Y S, Kim S Y et al. *International Journal of Precision Engineering and Manufacturing*[J], 2019, 20: 1563
- 22 Cheng J S, Wang Q L, Zhou F et al. *IEEE Transactions on Applied Superconductivity*[J], 2016, 26(7): 1
- 23 Stolyarov V V. *Journal of Machinery Manufacture and Reliability*[J], 2015, 44(4): 372
- 24 Zhao R L, Liu Y, Tian B H et al. *Heat Treatment of Metals*[J], 2011, 36(8): 17
- 25 Sun D, Jiang S Y, Yan B Y et al. *Journal of Alloys and Compounds*[J], 2020, 834: 155 010

## 基于模拟及实验的Cu/NbTi异温包覆挤压界面结合研究

孙冬<sup>1,2</sup>, 王哲<sup>3</sup>, 江树勇<sup>1,4</sup>, 张艳秋<sup>3</sup>

- (1. 先进金属复合材料成形技术与装备教育部工程研究中心, 山西 太原 030024)
- (2. 太原理工大学 机械与运载工程学院, 山西 太原 030024)
- (3. 哈尔滨工程大学 机电工程学院, 山西 太原 150001)
- (4. 太原理工大学 材料科学与工程学院, 山西 太原 030024)

**摘要:** 提出Cu/NbTi异温包覆挤压, 即在塑性变形过程中Cu和NbTi具有不同的温度。Cu/NbTi异温包覆挤压可以有效降低包覆层Cu的变形温度, 从而减小包覆层Cu和NbTi芯间的屈服应力差值, 有助于二者的协调变形。采用刚粘塑性有限元法模拟凹模入口角分别为60°, 120°和180°时Cu/NbTi异温包覆挤压过程, 揭示其界面结合情况。模拟结果表明, 增大凹模入口角有助于减小包覆层Cu和NbTi芯间的相对伸长量, 有益于二者的界面结合。根据有限元模拟优化的工艺参数, 进行了Cu/NbTi异温包覆挤压实验, 凹模入口角为180°。实验结果表明, 该条件下Cu/NbTi包覆挤压过程中金属稳定流动, 包覆层Cu和NbTi芯协调变形, 二者间相对伸长量较小。实验结果与模拟结果吻合较好。

**关键词:** 塑性变形; 挤压; NbTi合金; 有限元法

作者简介: 孙冬, 女, 1993年生, 博士, 太原理工大学机械与运载工程学院, 山西 太原 030024, E-mail: sundong01@tyut.edu.cn